https://doi.org/10.5194/se-2020-133
Preprint. Discussion started: 17 August 2020

Solid Earth Discussions

Emplacement of ”exotic“ Zechstein slivers along the inverted Sontra Graben (northern Hessen, Germany): clues from balanced cross-sections and geometrical forward modelling

Jakob Bolz[1], Jonas Kley[1]

[1]Department for Structural Geology & Geodynamics, Geoscience Centre, Georg-August-University, Göttingen, 37077, Germany

Correspondence to: Jonas Kley (jonas.kley@geo.uni-goettingen.de)

Abstract. Lens-shaped slivers of Permian (Zechstein) amid Triassic units, appearing along the main boundary fault of the Sontra Graben in central Germany on the southern edge of the Central European Basin System (CEBS) were studied by means of detailed map analysis, a semi-quantitative forward model and two balanced cross-sections. We show how partial reactivation of the graben's main normal fault and shortcut thrusting in the footwall during inversion, combined with a specific fault geometry involving flats in low shear-strength horizons, produce the observed slivers of ”exotic” Zechstein. Based on regional correlation, extension most likely occurred in Late Triassic to Early Cretaceous time while the contraction is of Late Cretaceous age. The kinematic history of the graben, reconstructed through field observations, structural and cross-section analysis is employed to discuss the dynamic evolution of the graben system in the immediate vicinity and to consider implications for the entire CEBS.

1 Introduction

The Mesozoic tectonic evolution of Central Europe involved long-lasting, Triassic to Early Cretaceous extension followed by a short-lived pulse of mostly Late Cretaceous contractional deformation. This history is best documented by subsidence and inversion in the main sub-basins of the Central European Basin System (CEBS) such as the Broad Fourteens and Lower Saxony basins and the Mid-Polish trough (Brochwicz-Lewinski & Pozarvski, 1987; Hooper et al., 1995; Mazur et al., 2005; Maystrenko & Scheck-Wenderoth, 2013). South of these basins a wide border zone of the CEBS also experienced first distributed extension of low magnitude and then equally dispersed contraction. These movements created an array of narrow grabens affected to different degrees by folding and thrusting. The grabens or fault zones are the most prominent structures in the otherwise flat-lying to gently dipping Mesozoic cover of the central German uplands (“Mittelgebirge”). They exhibit two prevailing strike directions: NW-SE and N-S to NNE-SSW, with the former considerably more frequent than the latter. The Sontra Graben discussed here is one of the NW-SE-trending Hessian Grabens. It is situated in the north-eastern part of the state of Hessen, approximately 50 km south of the city of Göttingen. The Hessian Grabens appear as narrow strips of Middle to Late Triassic (Muschelkalk and Keuper) strata, downfaulted by as much as several 100 meters relative to their Early Triassic

https://doi.org/10.5194/se-2020-133
Preprint. Discussion started: 17 August 2020

(Buntsandstein) surroundings. Many of them show a pronounced asymmetry, having one boundary fault with considerably larger displacement than the other. The structures of the graben interiors are highly variable, ranging from gentle synclines over successions of synclines and anticlines to rotated, fault-bounded blocks.

In the area of the Sontra Graben, Variscan metasedimentary basement consisting of Carboniferous and Devonian phyllites and greywackes (Motzka-Noering et al., 1987) is overlain by discontinuous Early Permian clastics and an originally continuous sequence of Latest Permian (Zechstein) through Triassic sandstones, shales, carbonates and evaporites. Numerous incompetent layers consisting mostly of sulfates and shales occur in the Zechstein strata and at two levels of the Triassic succession (Upper Buntsandstein and Middle Muschelkalk), but no thick halite was deposited (Fig. 1, 2, 3).

The Sontra Graben and several others exhibit enigmatic occurrences of Zechstein strata. The Zechstein rocks are found discontinuously as fault-bounded blocks or slivers/horses of Zechstein rocks along the faults of the grabens. These slivers of Zechstein carbonates are structurally elevated relative to both the graben interior and the bounding shoulders. In the Sontra Graben their dimensions vary from tens to several hundreds of meters long parallel to the strike of the graben and from meters to a few tens of meters wide perpendicular to it. Internally, the slivers appear almost undeformed. However, in most cases the bedding is moderately to steeply dipping and approximately fault-parallel.

It was previously suggested that the emplacement of the uplifted Zechstein blocks was due to salt diapirism (Lachmann, 1917). In the present paper we explore the hypothesis that they were emplaced as a result of inversion tectonics involving bedding-parallel decollements in two evaporitic Zechstein horizons during both extension and contraction.

2 Methods

2.1 Data sources

Data were compiled by detailed analysis of the official geological maps of the area (Beyrich & Moesta, 1872; Moesta, 1876; Motzka-Noering et al., 1987), maps from published thesis papers of the 1920s and 1930s (Bosse, 1934; Schröder, 1925) as well as unpublished maps created during two diploma mapping projects at the University of Jena (Brandstetter, 2006; Jähne, 2004). Dip and strike data were also gathered from numerous unpublished reports that were written for the beginner-level mapping courses in the years 2014 and 2015 at the University of Göttingen.

To complete the existing data, we visited all Zechstein slivers, the main focus of this study, along the length of the Sontra Graben, mapped their exact positions and extents and took dip readings where possible.

In recent years the area around the Sontra Graben was surveyed for the construction of a motorway which is now underway. In the course of this survey, numerous shallow wells were drilled. We used information from two of those to constrain the architecture of one fault hosting Zechstein slivers. Topography data for the cross sections were obtained from the topographic map of Hessen (1:25,000) and imported into Move (© Petroleum Experts) via the ASCII file import function. Topography data for the geological map were kindly provided by the Hessian Agency for Nature Conservation, Environment and Geology

https://doi.org/10.5194/se-2020-133
Preprint. Discussion started: 17 August 2020


Solid Earth Discussions

(HLNUG). Stratigraphic data (Fig. 2) were taken from Motzka-Noering et al., 1987, which contains a compilation of various well and outcrop data.

2.2 Workflow

The collected map data was digitised and georeferenced using QGIS (QGIS Development Team, 2015). All geological mapping was done using FieldMove (© Petroleum Experts) on an Apple iPad Air 2 and data from the app were fed into QGIS via the .csv import function. Subsequently, a new internally consistent geological map was constructed (Fig. 4). The resulting map and dip data from the aforementioned publications then served as the basis for modelling and cross-section construction in 2DMove (© Petroleum Experts). All data was fed into 2DMove via the shapefile (*.shp) or the ASCII (*.txt) import functions.

2.3 Cross-section construction and modelling

2.3.1 Forward structural model

The forward model was constructed in 2DMove (© Petroleum Experts) to test the viability of inversion-related emplacement of the Zechstein slivers. We constructed an undeformed layer cake model with horizontal bedding using the averaged stratigraphic thicknesses of the study area. For simplicity, the model contains only one fault which is assumed to represent the principal boundary fault of the Sontra Graben. Using the 2D-Move-on-Fault tool with the Simple Shear algorithm and 60° shear angle, we simulated normal fault displacement followed by reverse motion, adjusting the fault geometry and displacement magnitudes until a satisfactory approximation of the observed structures was reached. Finally, the 2D-Unfolding tool with the Simple Shear algorithm and a 60° shear angle was used to create folding of the section at greater wavelength.

2.3.2 Constructing the balanced geological cross-sections from map data

Both sections (Fig. 6) were constructed and balanced using 2DMove (© Petroleum Experts). From the dip data, an orientation analysis was conducted to determine the optimal orientation for the cross sections. Slickensides on fault surfaces and small-scale faults and folds associated with the Sontra Graben exhibit signs of shortening predominantly in a north-north-easterly direction. Hence, approximately plain strain deformation conditions for the profiles can be assumed for both the extensional and the contractional phase. All geological boundaries were derived from the newly compiled geological map, mentioned above. The 2D-Unfolding tool with a Flexural slip algorithm was used to flatten the folds, conserving bed lengths. The fault geometries were corrected through trial-and-error-cycles to prevent gaps or overlaps. Both sections were constructed in such a way that 3D implications by the fault geometry were considered and that a consistency and a continuity between the sections and along the graben was maintained.

Section A (Fig. 6) was positioned such that the cross-sectional plane coincides with the outcrop shown in Fig. 8, previously described by Schröder (1925), thus giving us an insight into the fault geometry of the graben and the way the Zechstein slivers

https://doi.org/10.5194/se-2020-133
Preprint. Discussion started: 17 August 2020

are juxtaposed with the graben shoulder and its interior. The outcrop shows one of the Zechstein slivers bounded on its south-south-westerly side by a thrust fault and on its north-north-easterly side by a normal fault. The Lower Muschelkalk adjacent to the Zechstein is internally folded. Further uphill the appearance of a second ”exotic” sliver of Middle Buntsandstein is likely linked to the normal fault in the NNE and could have been transported down during the extensional phase. Upon inversion, together with the Zechstein, it was raised to its current position.

3 Results

3.1 Structural segmentation of the Sontra graben

The NW-SE-trending Sontra Graben extends for a length of 35 km between the N-trending Altmorschen-Lichtenau-Graben in the west and the northwestern tip of the Thuringian Forest, a fault-bounded basement anticline in the east (Fig. 1). On both ends the Sontra Graben is reduced to a single fault before linking up with the other structures. Near its centre, the Wellingerode Graben splays from the Sontra Graben and runs first north-northeastward and then in a more northeasterly direction to meet the NW-SE-trending Netra Graben.

The main part of the Sontra Graben within the study area is subdivided into five segments for the purpose of this paper (Fig. 4). In the very northwest (segment I) the Graben has a width of approximately 500 metres. It is confined between two major faults, both with vertical offsets around 150 to 180 metres. Zechstein slivers occur at both faults and are comparatively small (from 1.000 to 16.000 m^2, Table 1 for comparison).

Further to the southeast, segment II comprises a short stretch of graben near the village of Stadthosbach, where it becomes quite narrow (250 metres). The Graben continues to show two main faults with small-sized Zechstein slivers at the southwestern fault. Vertical offset amounts to no more than 80 metres. The comparatively narrow width could be an artefact of topography. At this point, a small river has incised a 100-metre-deep valley at a right angle to the graben, which could explain a narrower outcrop, assuming that the graben becomes narrower with depth.

Segment III is strongly influenced by interference with the Wellingerode Graben. The Sontra Graben reaches a width of up to 1.2 kilometres and shows first hints at a southeast trending axial syncline, in certain parts well silhouetted by the Trochitenkalk formation. of the Upper Muschelkalk. The Lower Muschelkalk outcrop becomes very broad in this part of the graben probably due to fault repetition (see also Fig. 9). The aforementioned axial syncline interferes with the Wellingerode Graben in this segment. West of the Mühlberg hill, a fold interference pattern is developed, formed by superposition of the NW- and NNE-trending synclines associated with the Sontra and Wellingerode grabens, respectively. No Zechstein slivers are present in this part of the graben.

East of the Mühlberg mountain, segment IV comprises the largest Zechstein slivers that appear exclusively along the southwestern border fault. The graben, again, is very narrow (110 metres), at the point where the river Sontra transects it. In the north-eastern part of segment IV, tilted blocks of Lower Muschelkalk surrounded by Upper Buntsandstein shale appear, while open folding is the dominant structural style in its southwestern part where the axial syncline becomes quite prominent.

https://doi.org/10.5194/se-2020-133
Preprint. Discussion started: 17 August 2020

These apparently lateral variations in structural style along the graben more likely are expressions of different vertical styles obscured by the effects of topography. We interpret this vertical contrast as an effect of decoupling, occurring between the Lower and the Upper Muschelkalk due to the low competence of the mainly marl bearing Middle Muschelkalk. All units below the Middle Muschelkalk exhibit a block style deformation and rotation, dominated by faulting, whereas units above the Middle Muschelkalk more frequently produce axial folds (Fig. 9).

In segment V, the graben widens to more than two kilometres and also changes direction slightly to a more south-southwesterly trend, skirting the southern edge of the Ringgau, a topographically elevated panel of flat-lying Muschelkalk strata between the Sontra Graben and the Netra Graben. Large-scale folding gives way again to block-faulting and tilting as dominant structural style. Small Zechstein slivers occur on several faults of the graben interior but are restricted to the northwestern part of the segment.

3.2 Mechanical stratigraphy

In Late Permian times, the Zechstein transgression flooded the Southern Permian Basin from the central North Sea into western Poland and from the southern margin of the Baltic shield in the north to the Rhenish massif and the Bohemian massif in the south (Fig. 10) (Ziegler, 1990). The Zechstein sediments were deposited as seven recurring cycles (Richter-Bernburg, 1953) comprising clastic sediments at the base, overlain by carbonates, sulphates, halites and potash/magnesium salts in only some parts of the basin (Becker & Bechstädt, 2006). Situated on the southern edge of the Southern Permian Basin, the study area mainly comprises the first three Zechstein cycles, termed the Werra, Staßfurt and Leine (or Z1 to Z3) cycles and contains the subsequent four cycles only in a shaly marginal facies. The basin-margin character of the region resulted in original Zechstein thicknesses in parts as low as 60 metres in the study area. From a mechanical viewpoint, the Zechstein constitutes a relatively thin but very heterogeneous succession of alternating competent and incompetent packages. The strongest units are the carbonates of the Z2 and Z3 cycles, traditionally termed “Hauptdolomit” (main dolomite, Ca2) and “Plattendolomit” (platy dolomite, Ca3). The Zechstein found as slivers in the Sontra Graben typically consists of poorly bedded to massive vuggy (cellular) dolomite, a facies that occurs in both the Ca2 and Ca3 carbonates.

Prominent weak layers and therefore potential detachment horizons are the evaporites and shales. The Ca2 carbonate is underlain by thick sulfate and shale of the Z1 cycle, termed the Werra anhydrite (A1) and Braunroter Salzton (brownish red salty clay, T1r). T1r consists of up to 4-metre-thick greyish-green, thin-layered shales originally interspersed with thin layers of halite. There is no indication of primary massive rock salt in Z1 of the study area. Above the Ca2 carbonate and separating it from Ca3 there is another shale horizon. Again, there is no indication for salt deposition during Z2 in this part of the basin. The Ca3 carbonate is either overlain by anhydrite (A3) or grey, clayey carbonates (Ca3T). Near the town of Sontra, the A3 anhydrite level is exposed as relatively homogeneous gypsites with thin (1 cm) layers of brownish dolomite. Traditionally, the term “Obere Letten” (upper clays) was used as a collective term for claystones, siltstones and sandstones of small thickness overlying Ca3 or A3 and belonging to the Leine and higher cycles (Z3 to Z7).

https://doi.org/10.5194/se-2020-133
Preprint. Discussion started: 17 August 2020

The Z3 to Z7 shales grade upwards into the Triassic Buntsandstein via a succession of siltstones. The Triassic succession also comprises three competent units: the mostly sandy and competent Lower and Middle Buntsandstein, the Lower Muschelkalk and the lower part of the Upper Muschelkalk (Trochitenkalk Fm.). Potential detachment horizons between them are formed by the evaporitic and shaly Upper Buntsandstein and the evaporitic and marly Middle Muschelkalk. The higher part of the Upper Muschelkalk and Keuper represent an incompetent stratal package at the top of the column.

3.3 Forward Model

The forward structural modelling helped us to better constrain the possible geometry of the Sontra Graben main fault and its role in the formation of the Zechstein slivers. It was particularly useful in exploring the influence of decollements in the incompetent rock units and provided guidance in the construction of the two balanced cross-sections. The fault of the final model has an overall listric geometry with a dip angle of 60° at the surface that becomes a low-angle detachment at a depth of 800 metres within the Werra anhydrite (Fig. 5a). The listric geometry is broken by three flats or short detachments, sitting in the Middle Muschelkalk, the Upper Buntsandstein and the main anhydrite (A3) of the Zechstein. An extension of approximately 1.2 kilometres is sufficient to bring the Lower Muschelkalk of the hanging wall to the depths of the Zechstein when assuming a listric fault geometry. A flat in the “Hauptanhydrit” (main anhydrite, A3) creates a step in the fault geometry, which upon inversion promotes the formation of a shortcut thrust, allowing for the creation of a Zechstein horse. For the inversion phase, a shortcut thrust was introduced (Fig. 5b) creating a Zechstein horse with the original normal fault as a roof thrust and the newly created shortcut thrust as a sole thrust (Fig. 7a). A backthrust (Fig. 7b) was also created and the Zechstein horse emplaced onto the underlying Lower Muschelkalk of the hanging wall. This was included into the model to provide an explanation for the fact that in one of the wells, the Zechstein was found to overlie the Lower Muschelkalk. Shortening of approximately 1000 metres sufficed to elevate the newly created Zechstein sliver to a regional stratigraphic level within the Upper Buntsandstein, a level where such slivers are commonly found along the Graben. Finally, the 2D-Unfolding tool with the Simple Shear algorithm and a 60° shear angle was used to create folding of a greater wavelength of about 1.5 kilometres, a feature that is also observed in the field.

Producing a new thrust fault, instead of reactivating the original normal fault, requires a steep fault-angle at a close distance to the basal detachment. Flats in low shear-strength layers were also observed in other grabens in the general area (Arp et al., 2011).

After its formation, further contraction of the graben results in the Zechstein horse being thrust onto the hanging wall and ultimately becoming elevated to the observed stratigraphical position. Flats in the Intermediate Muschelkalk and the Upper Buntsandstein were merely incorporated to acknowledge their similar behaviour to the anhydrite-bearing Zechstein horizons, due to comparable physical properties. They do not, however play any further role in the structural evolution of the model. Shortening of approximately 1.2 km is necessary to elevate the sliver into the stratigraphical positions that are observed in the field.

https://doi.org/10.5194/se-2020-133
Preprint. Discussion started: 17 August 2020


Solid Earth Discussions

3.1 Balanced Cross-sections

3.1.1 Cross-section 1: Mühlberg

Cross-section A (Fig. 6) shows a long-wavelength syncline, striking parallel to the Sontra Graben. The graben itself has a width of only 150 metres in this section. At the surface the main boundary fault in the southwest dips to the northeast at an almost vertical angle, following a listric geometry down to the depth of the Werra-Anhydrite. There, it curves slightly upward, parallel to bedding, to form a horizontal decollement at a depth of approximately 300 metres below the surface. A second fault appears as a backthrust dipping towards the southwest and ending at the boundary fault at a depth of 50 metres below the surface. The central block in the graben is backthrust over the north-eastern shoulder and appears stratigraphically lowered relative to the southwestern shoulder.

Two fault bounded slivers of Zechstein and Middle Buntsandstein appear parallel to the main boundary fault. At shallow depth, they are cut off by the backthrust fault.

Due to the deformation associated with the long-wavelength syncline, fault angles and geometries of the graben faults appear somewhat unintuitive.

3.1.2 Cross-section 2: Weißenborn

At the location of cross-section B (Fig. 6), the Graben has a width of approximately 370 metres. The NW-trending long-wavelength syncline continues well visible in this section. A flexure in the hanging wall does not exist. The boundary fault in the southwest dips at an angle of approximately 70° towards the northeast and flattens out to become a horizontal decollement at a depth of approximately 450 metres. The backthrust has a similar geometry as in section 1, dipping towards the SW at an angle of approximately 45° and flattening out, parallel to bedding in the centre of the graben.

This section cuts through the largest of the Zechstein slivers. Again, it is cut off at a shallow depth by the backthrust.

3.1.3 Transfer structure

Map analysis shows that west of section A the occurrence of the Zechstein slivers along one single main inverted thrust changes to a different pattern, in which a double-row of the slivers along a series of imbricated faults prevails. We suggest these faults function as part of a transfer structure, where the seemingly disconnected individual faults link up at depth conjoining into one single detachment (Fig. 11). Said fault geometry could comfortably facilitate the previously developed model (Fig. 7) for explaining the emplacement of the Zechstein slivers in this particular configuration. We also show how erosion functions as the main controlling mechanism for determining the width of the graben at the surface, where advanced erosion leaves only a narrow band of fault-bounded Zechstein.

https://doi.org/10.5194/se-2020-133
Preprint. Discussion started: 17 August 2020

3.2 Summary of the structural interpretation

A comparison of the two cross-sections clearly demonstrates the widening of the Graben towards the southeast. In both sections, long wave-length folding overprints the original geometry of the listric normal boundary fault and its inversion features, such as the backthrust fault and thus fault angles become somewhat skewed. The sections also expose that the features, which can be observed at the surface are in fact the mere roots of a graben, whose main body has already been eroded. The forward model constitutes the main basis for the construction of the balanced cross-sections, since few other constraints, especially for the fault geometry exist.

3.4 Formation of the Backthrust

Well data from 20 metres to the northwest of the profile line indicate that at least at one location Zechstein is thrust on top of the Lower Muschelkalk of the hanging wall at a shallow depth of approximately 30 metres. Backthrusts are a well-documented feature of inverted grabens (Hayward & Graham, 2015). A kinematically viable solution would therefore be a backthrusting movement of the Zechstein horse onto the Lower Muschelkalk of the hanging wall.

3.5 Exotic Zechstein Slivers

The Zechstein slivers that crop out along the graben vary greatly in size and shape. A trend towards larger, more continuous slivers can be observed from the northwest to the southeast, i.e. from segment I to V (Table 1, Fig. 4). The Lower Muschelkalk appears most commonly as bordering unit on the south-western side of the slivers while in the north-east, the slivers are generally bordered on by the Upper Buntsandstein. Assigning a stratigraphical unit to the individual outcrops can prove difficult. Although most of the slivers actually produce conspicuous rocky outcrops and it is generally even possible to measure the bedding dips, they often consist of poorly bedded to massive, vuggy (cellular) dolomite, a facies that occurs in both the Hauptdolomit (Z2, Staßfurt cycle) and Plattendolomit (Z3, Leine cycle) carbonates (Fig. 3). In addition, weathering has greatly altered their colour, rendered bedding unrecognizable or in some cases has decomposed the rock to a powdery ash-like substance.

4 Discussion

In the two balanced cross-sections and the forward model, we showed that the emplacement of exotic Zechstein slivers into higher stratigraphic levels by inversion of the graben's boundary fault is geometrically possible.

Earlier workers, like Lachmann (1917) suggested salt tectonics as a way to produce the slivers. A salt diapir, intruding into the suprasalt succession and dragging the suprasalt Zechstein with it, was hypothesized to have been dissolved and to have only left behind remnants of the carbonates that originally enveloped it. However, since the primary salt thickness in the area of the Sontra Graben was very small (Motzka-Noering et al., 1987), this seems an unlikely interpretation.

https://doi.org/10.5194/se-2020-133
Preprint. Discussion started: 17 August 2020


Solid Earth Discussions

4.1 Fault geometries

Apart from the general rules of mechanical stratigraphy the existence of such flats in incompetent horizons is based on field observations, made by Arp, Tanner and Leiss, 2011 and Möbus, 2007 on normal faults that are associated with the Leinetal Graben, circa 40 kilometres north of the study area.

According to the Mohr-Coulomb fracture criterion, upon inversion, a new shortcut thrust fault is only likely to form, if the original normal fault is significantly steeper than 30° relative to a subhorizontal σ_1 (thrust regime). However, if we assume a listric fault geometry for the original normal fault with a basal detachment in the Hauptanhydrit (main anhydrite, A3) at such close distance above the basal detachment, the fault-angle should not be very high and thus a reactivation of the normal fault, without producing any slivers appears more likely.

Therefore, the formation of flats in low shear-strength horizons on the original normal fault during the extensional phase plays a key role in my model for the creation of the Zechstein slivers. Without the flats, the angle of the normal fault near the basal decollement would not be steep enough to induce the formation of shortcut thrusts, necessary to create a horse between the normal fault and the newly developed shortcut thrust (Fig. 7).

For this model, we assumed that immediately below the flat, the fault returns to a dip of 60° a typical angle for normal faults, and then flattens out again towards the following flat and eventually towards the basal detachment.

The geometry of the fault plays a key role in the formation and shape of the Zechstein slivers. In particular, the length of the flat and its height above the basal detachment are the main factors that control the final geometry of the observed Zechstein slivers, whereas height above the basal detachment controls their thickness.

Given that the vertical distance between the top Hauptanhydrit and the top Werra-Anhydrit around the Sontra Graben is only between 60 and 80 metres, the total thickness of a sliver cannot exceed this value.

Another important feature, which was observed in the field, is the superimposition of “exotic” Zechstein over Lower Muschelkalk which is most likely part of the hanging wall. We therefore suggest backthrusting of the Zechstein sliver onto the Muschelkalk during inversion (Fig. 5, 6).

Thrusting is likely to have occurred during early stages of the inversion phase. The forward model suggests that a probable geometric constellation with conditions suited to induce back-thrusting is immediately following the onset of inversion. In this constellation, the main original normal fault is at a particularly high angle and contractional movement on this fault would cause considerable stress in the adjoining hanging wall and footwall, triggering the backthrusting of the Zechstein sliver onto the hanging wall to a certain extent. Subsequently, the Zechstein horse, bounded at the top by the original normal fault and at the base by the newly created (shortcut) thrust fault and backthrust fault, could be carried to its present-day stratigraphic level.

The choice of algorithm for the forward model had little effect on the outcome. MOVE offers a limited choice of algorithms that are suited for the modelling of normal faults. Running the simulation with either the Fault Parallel Flow algorithm or the Simple Shear algorithm proved to have little effect on the amount of extension required to lower the hanging wall Lower

https://doi.org/10.5194/se-2020-133
Preprint. Discussion started: 17 August 2020

Muschelkalk to the depth of the lower Zechstein detachment This demonstrates a certain robustness of the model and the assumptions therein.

4.2 The Zechstein as a Detachment Horizon

The model is based on the assumption that a detachment in the Zechstein is possible. Were the initial normal fault of the graben to cut straight through to the basement, it would seem unlikely that upon inversion a newly created shortcut thrust would lead to the observed geometries. Any such fault would most likely, if any, produce slivers of basement rock. The Zechstein succession with its multiple evaporite layers appears prone to forming detachment horizons, similar to the decoupling of the sedimentary cover from the basement along evaporites that is extensively documented for the extensional fault systems at the passive margins of the Gulf of Mexico and Brazil (Adam et al., 2012; Demercian et al., 1993; Duval et al., 1992).

It has been suggested by Mazur, Scheck-Wenderoth and Krzywiec (2005) that detachment horizons in the Zechstein also occur in the North German Basin, a sub-basin of the CEBS. Nonetheless, one should take into consideration the facies changes within the CEBS. The NGB lies much further to the north than the Hessian Grabens and has considerably thicker Zechstein.

Another significant difference between a salt-bearing passive margin and the CEBS is the absence of a strong topographic gradient towards an ocean basin. The topographic gradient, however, constitutes the main driving mechanism for downhill sliding over a detachment horizon in the cases of passive margins. A different driving mechanism is therefore required for the CEBS.

Basement up-thrusts like the Harz Mountains or the Thuringian Forest could certainly drive deformation in the sedimentary layer, at least for compressional forces. The exhumation ages of the Harz Mountains (Voigt et al., 2008) coincide with the proposed time of the graben inversion. Thus, it would seem plausible for deformation in the basement to occur elsewhere in or on the edge of the basin and for the sedimentary cover to act more or less independently.

For the preceding extensional phase, however, traces of a similar extension in the basement have yet to be found. It is possible that, similar to the Sontra Graben, a previous graben structure in the basement has simply been reset to its original regional elevation. The small net offset and the fact that the fault is likely to be covered by sediments would certainly obscure its character as an extensional structure. Given that countless structures throughout the CEBS were reactivated during Iberia-Europe convergence, it seems almost unlikely to find any large basement structure that has not been affected by the contractional push.

4.3 Distribution of “exotic” slivers

The question why the Zechstein slivers only occur on some grabens remains a key issue. The Sontra Graben is in close proximity to the Netra Graben. Yet, no ”exotic” slivers, Zechstein or otherwise, can be observed in the latter. It is possible that a special paleo-geographic configuration gave rise to this kind of phenomenon. Notably, all ”exotic” Zechstein slivers appear on two relatively discrete bands near the southern edge of the Z1 basin (Fig. 10) and predominantly originate from its carbonate shelf with the exception of localities 1 and 2, relatively small specimen, which originate from the sulphate slope. The area of

https://doi.org/10.5194/se-2020-133
Preprint. Discussion started: 17 August 2020

the Sontra Graben is also situated just on the northeastern edge of the Schemmern-Swell and close to the centre of the Waldkappel Depression, two paleogeographic features of the Z1 basin (Kulick et al., 1984). This could have produced a special facies-type with physical properties that might favour this kind of structure, most likely an alternation of strong carbonate layers and evaporites that are thick enough to act as detachments but too thin to form proper salt structures (pillows and diapirs). In order to test this hypothesis, a comparative study of all the structures in which exotic slivers occur would have to be made with special focus on their paleogeographic setting.

Another possibility is extension in the Netra Graben simply did not suffice to bring the Lower Muschelkalk as far down as the Zechstein. A theory, supported by the fact that Zechstein does not appear in any immediate vicinity of the Netra Graben. During the contractional phase, the formation of shortcut thrusts in the Sontra Graben will have released some of the stress on the graben system and strain on the Netra Graben's footwall might have been insufficient to produce shortcut thrusts.

4.4 Timing of the Deformation Phases

Since such a significant portion of the graben has been eroded and only its roots remain, it is not possible to directly infer a deformation age due to the lack of syn-rift and post-rift sediments. However, the fact that Upper Triassic units (Muschelkalk and Lower Keuper) are in fault contact with Lower Triassic units (Buntsandstein) requires the deformation to have occurred after the deposition of the Lower Keuper.

Graben inversion, typically recognizable through stratigraphic constraints such as the thickening of the syn-rift sediments towards the boundary fault (Williams et al., 1989), cannot be proven by these means, again due to the lack of syn-rift deposits. Another way to recognize inversion on a map is through faults that, following the strike of the graben, change from normal to thrust fault (Williams et al., 1989). This is clearly the case with the Sontra Graben (Fig. 4). Finally, the position of the Zechstein slivers can be seen as evidence for graben inversion, when the assumptions of the forward model are accepted.

The timing for the extension and contraction of the different graben directions, Sontra Graben and Netra Graben versus Wellingerode Graben, poses another difficult question. Generally, it can be said that the Wellingerode Graben appears to terminate at both the Sontra Graben and the Netra Graben. Using an analogy from joint propagation (Engelder, 1985), this would imply that the Sontra Graben and Netra Graben already existed when the Wellingerode Graben formed, releasing its tension once their boundary faults had connected.

Previous authors (Vollbrecht et al. in Leiss *et al.*, 2011) have suggested a dextral strike-slip regime for Lower Saxony and Northern Hessen and the simultaneous formation of the grabens in both direction (NW-striking and NNE-striking). This however, would imply a considerable amount of strike-slip motion along the boundary faults of all three grabens. Field observations made during this study do not support that hypothesis.

https://doi.org/10.5194/se-2020-133
Preprint. Discussion started: 17 August 2020


Solid Earth
Discussions
Open Access
EGU

5 Conclusions

The Sontra Graben is one of the many NW-trending structures in the CEBS. It displays unambiguous signs of both extension and contraction.

Variations in structural style along the graben are the basis for distinguishing five segments. To the northwest, segment I shows one major boundary fault in the southwest with many small “exotic” slivers and a second possibly conjugate fault in the northwest. Segment II comprises the narrowest part of the graben and the transition from fault dominated blocks to the emersion of a longer wave-length central syncline. Segment III is dominated by the intersection of the Wellingerode Graben. The central synclines of the Sontra Graben and the Wellingerode Graben form a cumulative structure. Zechstein slivers do not appear in this segment. Segment IV is dominated by fault-bounded and rotated blocks in the northwest and contains the longest continuous Zechstein sliver. Segment V shows the widening of the graben and the continuation of the syncline.

The Sontra graben exhibits an unusually high number of “exotic” Zechstein slivers of varying size. The slivers are lenses of carbonates, up to several hundred metres in length, emplaced along the main graben faults to a structural position higher than either the graben interior or the shoulders. The geometry of the Zechstein slivers suggests that they formed via shortcut thrusts dissecting a stepped normal fault with ramps and flats. Backthrusts locally emplaced the slivers over the hanging wall. Forward modelling indicates that extension must have occurred prior to contraction, thus conforming with the tectonic evolution of Central Europe in the Mesozoic. For the extensional and contractional phase, maximum values of approximately 1.2 kilometres of horizontal extension/shortening were determined.

The overall structural style of the Sontra graben is suggestive of thin-skinned tectonics with a detachment horizon in the Werra Anhydrite of the lowest Zechstein cycle. At sub-Zechstein level, shortening was probably accommodated in the inverted Rotliegend basin of the Richelsdorf mountains to the south. Both regions were kinematically linked by the Zechstein detachment. and the expression of the respective basement deformation.

https://doi.org/10.5194/se-2020-133
Preprint. Discussion started: 17 August 2020

References

Adam, J., Ge, Z., & Sanchez, M. (2012). Salt-structural styles and kinematic evolution of the Jequitinhonha deepwater fold belt, central Brazil passive margin. *Marine and Petroleum Geology*, *37*(1), 101–120. https://doi.org/10.1016/j.marpetgeo.2012.04.010

Arp, G., Tanner, D., & Leiss, B. (2011). Struktur der Leinetalgraben-Randstörung bei Reiffenhausen. In *Neue Untersuchungen zur Geologie der Leinetalgrabenstruktur* (pp. 17–21).

Becker, F., & Bechstädt, T. (2006). Sequence stratigraphy of a carbonate-evaporite succession (Zechstein 1, Hessian Basin, Germany). *Sedimentology*, *53*(5), 1083–1120. https://doi.org/10.1111/j.1365-3091.2006.00803.x

Beyrich, E., & Moesta, F. (1872). *Erläuterungen zur geologischen Specialkarte von Preussen und den Thüringischen Staaten, Blatt Sontra*.

Bosse, H. (1934). Tektonische Untersuchungen an niederhessischen Grabenzonen südlich des Unterwerrasattels. *Abh. Des Preuß. Geolog. Landesamtes*, *Neue Folge*, 1–37.

Brandstetter, A. (2006). *Der nordwestliche Sontra-Graben, Unpublished diploma mapping project report*. University of Jena.

Brochwicz-Lewinski, W., & Pozarvski, W. (1987). The Mesozoic and Tertiary evolution of the Polish Trough. *Elsevier Science Publishers B.V*, *137*(43), 43.

Demercian, S., Szatmari, P., & Cobbold, P. R. (1993). Style and pattern of salt diapirs due to thin-skinned gravitational gliding, Campos and Santos basins, offshore Brazil. *Tectonophysics*, *228*(3–4), 393–433. https://doi.org/10.1016/0040-1951(93)90351-J

Duval, B., Cramez, C., & Jackson, M. P. A. (1992). Raft tectonics in the Kwanza Basin, Angola. *Marine and Petroleum Geology*, *9*(4), 389–404. https://doi.org/10.1016/0264-8172(92)90050-O

Engelder, T. (1985). Loading paths to joint propagation during a tectonic cycle: an example from the Appalachian Plateau, U.S.A. *Journal of Structural Geology*, *74*(3), 459–476.

Hayward, A. B., & Graham, R. H. (2015). Some geometrical characteristics of inversion. *Geological Society, London, Special Publications*, (44), 17–39.

Hooper, R. J., Goh, L. S., & Dewey, F. (1995). The inversion history of the northeastern margin of the Broad Fourteens Basin. *Geological Society, London, Special Publications*, *88*(1), 307–317. https://doi.org/10.1144/gsl.sp.1995.088.01.17

Jähne, F. (2004). *Der Sontra-Graben, NE-Teil, Unpublished diploma mapping project report*. University of Jena.

Kiersnowski, H., Paul, J., Peryt, T. M., & Smith, D. B. (1995). Facies, Paleogeography, and Sedimentary History of the Southern Permian Basin in Europe. *The Permian of Northern Pangea*, 119–136. https://doi.org/10.1007/978-3-642-78590-0_7

Kley, J. (2013). Saxonische Tektonik im 21. Jahrhundert. *Zeitschrift Der Deutschen Gesellschaft Für Geowissenschaften*, *164*(2), 295–311. https://doi.org/10.1127/1860-1804/2013/0022

Kulick, J., Leifeld, D., & Meisl, S. (1984). Petrofazielle und chemische Erkundung des Kupferschiefers der Hessischen Senke

https://doi.org/10.5194/se-2020-133
Preprint. Discussion started: 17 August 2020

395 und des Harz-Westrandes. *Geologisches Jahrbuch Reihe D*, *D 68*, 223.

Lachmann, R. (1917). Ekzeme und Tektonik. *Zentralbl. f. Min. Usw*, *414*.

Leiss, B., Tanner, D., Vollbrecht, A., & Arp, G. (2011). *Neue Untersuchungen zur Geologie der Leinetalgrabenstruktur*. Universitätsdrucke Göttingen.

Maystrenko, Y. P., & Scheck-Wenderoth, M. (2013). 3D lithosphere-scale density model of the Central European Basin
400 System and adjacent areas. *Tectonophysics*, *601*, 53–77. https://doi.org/10.1016/j.tecto.2013.04.023

Mazur, S., Scheck-Wenderoth, M., & Krzywiec, P. (2005). Different modes of the Late Cretaceous–Early Tertiary inversion in the North German and Polish basins. *International Journal of Earth Sciences (Geologische Rundschau)*, *94*, 782–798. https://doi.org/10.1007/s00531-005-0016-z

Möbus, H.-M. (2007). Die Hessischen Gräben als mehrfach duktil entkoppelte "pull apart"-Strukturen. *Geol. Jb. Hessen*, *135*,
405 2–23.

Moesta, F. (1876). Erläuterungen zur geologischen Specialkarte von Preussen und den Thüringischen Staaten, Blatt Waldkappel.

Motzka-Noering, R., Anderle, H.-J., Blum, R., Diederich, G., Grundlach, H., Hentschel, G., et al. (1987). Geologische Karte von Hessen 1:25000 Erläuterungen, Blatt 4925 Sontra, (2. Aufl.).

410 QGIS Development Team. (2015). QGIS Geographic Information System.

Richter-Bernburg, G. (1953). Stratigraphische Gliederung des deutschen Zechsteins. *Zeitschrift Der Deutschen Geologischen Gesellschaft*, *105*, 843–854.

Schröder, E. (1925). Tektonische Studien an niederhessischen Gräben. *Abh. Des Preuß. Geolog. Landesamtes*, *Neue Folge*, 57–82.

415 Voigt, T., Reicherter, K., von Eynatten, H., Littke, R., Voigt, S., & Kley, J. (2008). Sedimentation during basin inversion. In S. N. R. Littke, U. Bayer, D. Gajewski (Ed.), *Dynamics of Complex Sedimentary Basins. The Example of the Central European Basin System* (pp. 211–232). Berlin Heidelberg: Springer-Verlag.

Williams, G. D., Powell, C. M., & Cooper, M. A. (1989). Geometry and kinematics of inversion tectonics. *Geometry and Kinematics of Inversion Tectonics*, (44), 3–15. https://doi.org/10.1144/GSL.SP.1989.044.01.02

420 Ziegler, P. . (1990). *Geological Atlas of Western and Central Europe (2nd Edition)*. Shell Internationale Petroleum Mij. BV and Geological Society of London (London).

https://doi.org/10.5194/se-2020-133
Preprint. Discussion started: 17 August 2020

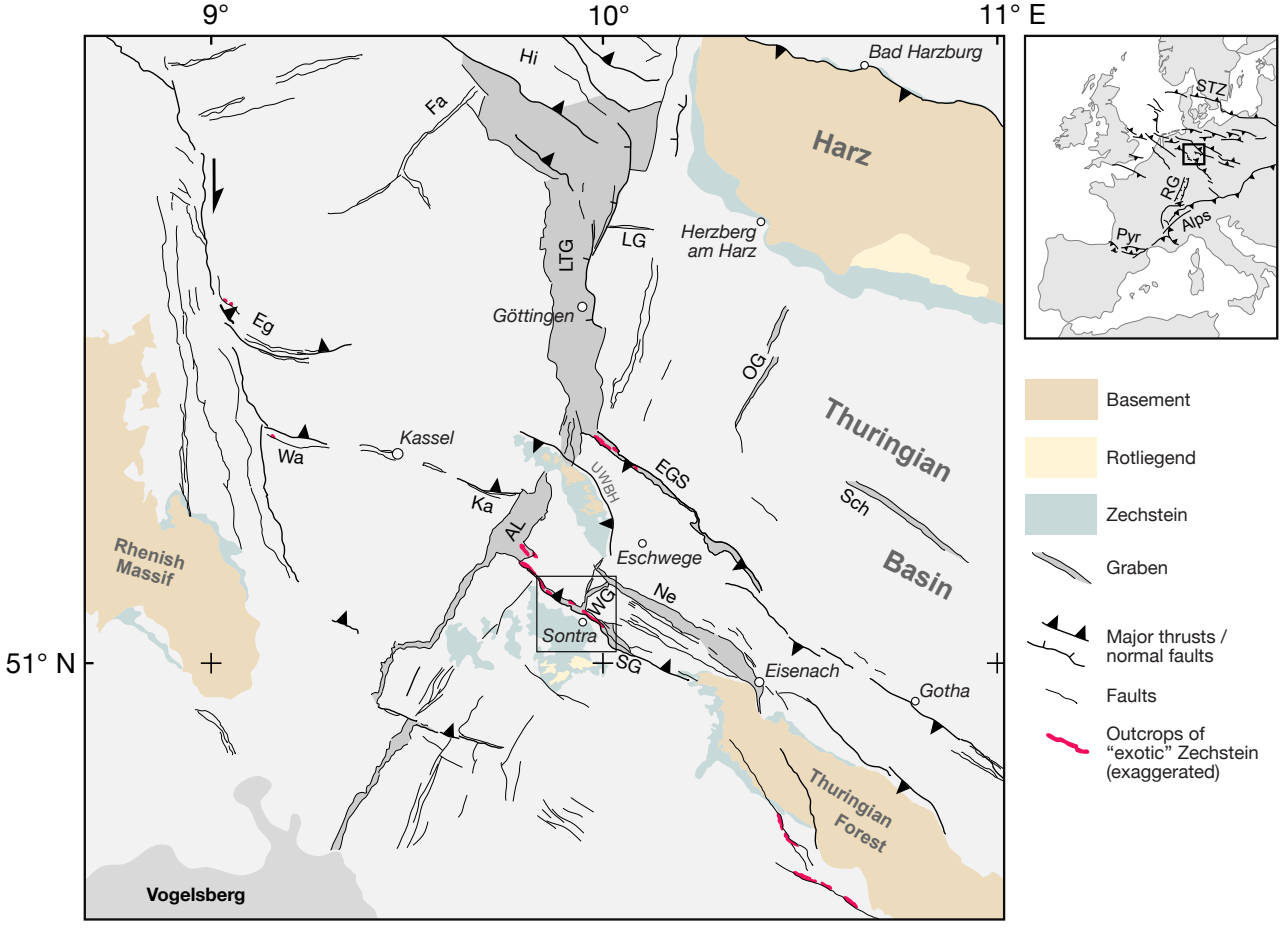

425

Figure 1: Basin architecture of the southern extent of the Central European Basin System (CEBS). Modified from Kley (2013) and the sources indicated therein. Paleogeography is derived from Ziegler (1990). The major Mesozoic and Cenozoic structural elements of the basin are shown. The black box indicates the study area, shown in greater detail in Fig. 4.

Abbreviations: AL = Altmorschen Lichtenau Graben, Eg = Egge, EGS = Eichenberg Gotha Saalfeld Fault,
430 **Fa = Falkenhagen Fault Zone, Hi = Hils Mulde, Ka = Kasseler St^rungszone, LG = Langfast Graben, LTG = Leinetalgraben, Ne = Netragraben, OG = Ohmgebirgegraben, RM = Richelsdorf Mountains, Sch = Schlotheimer Graben, UWBH = Unter Werra Basement High, Wa = Warsteiner St^rungszone WG = Wellingerodegraben**

https://doi.org/10.5194/se-2020-133
Preprint. Discussion started: 17 August 2020

Solid Earth
Discussions
Open Access
EGU

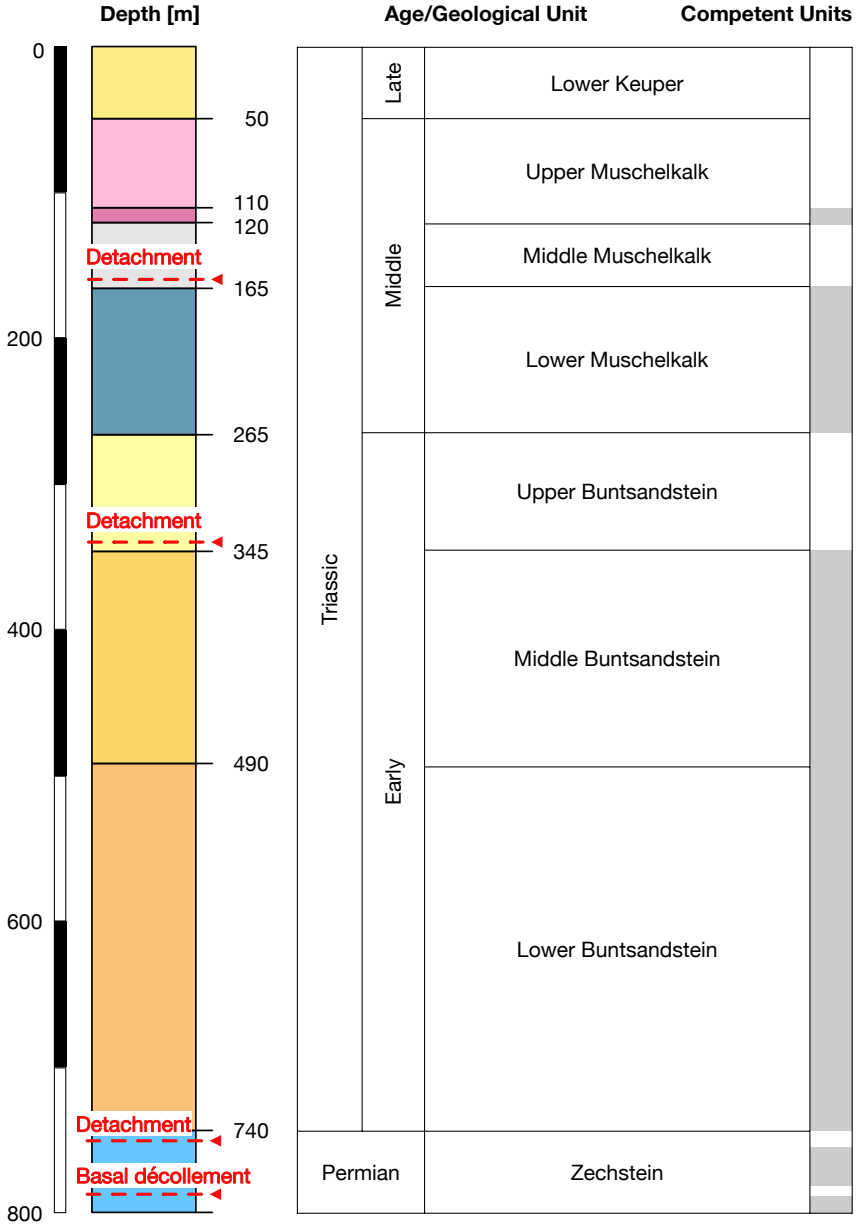

Figure 2: Stratigraphic column across the sedimentary cover within the study area. Major detachment horizons and the basal décollememt are indicated. Competent horizons are highlighted in grey.

https://doi.org/10.5194/se-2020-133
Preprint. Discussion started: 17 August 2020

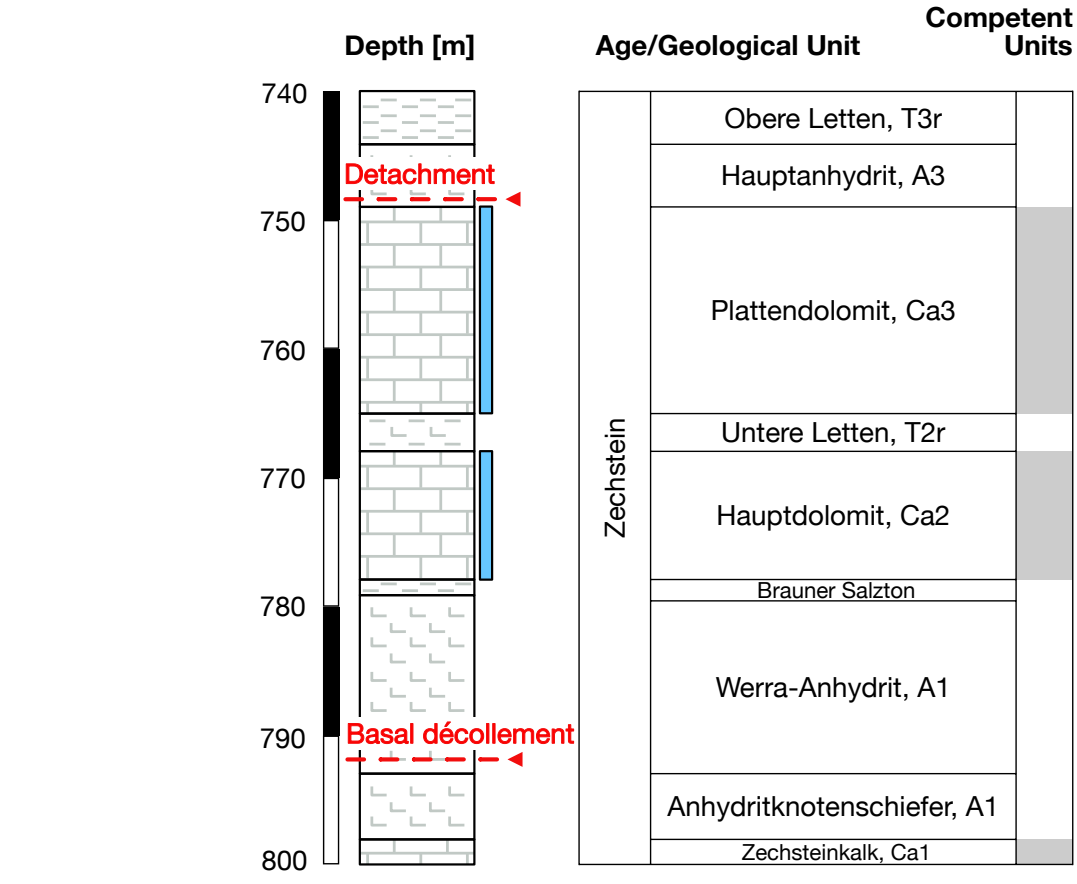

Figure 3: Detailed Stratigraphic column of the Zechstein Formation. Dolomite bearing horizons, which produce the majority of the "exotic" fragments are indicated in blue. The Hauptanhydrit and the Werra-Anhydrit form the most likely detachment horizons. Zechstein nomenclature after Richter-Bernburg, 1953.

https://doi.org/10.5194/se-2020-133
Preprint. Discussion started: 17 August 2020

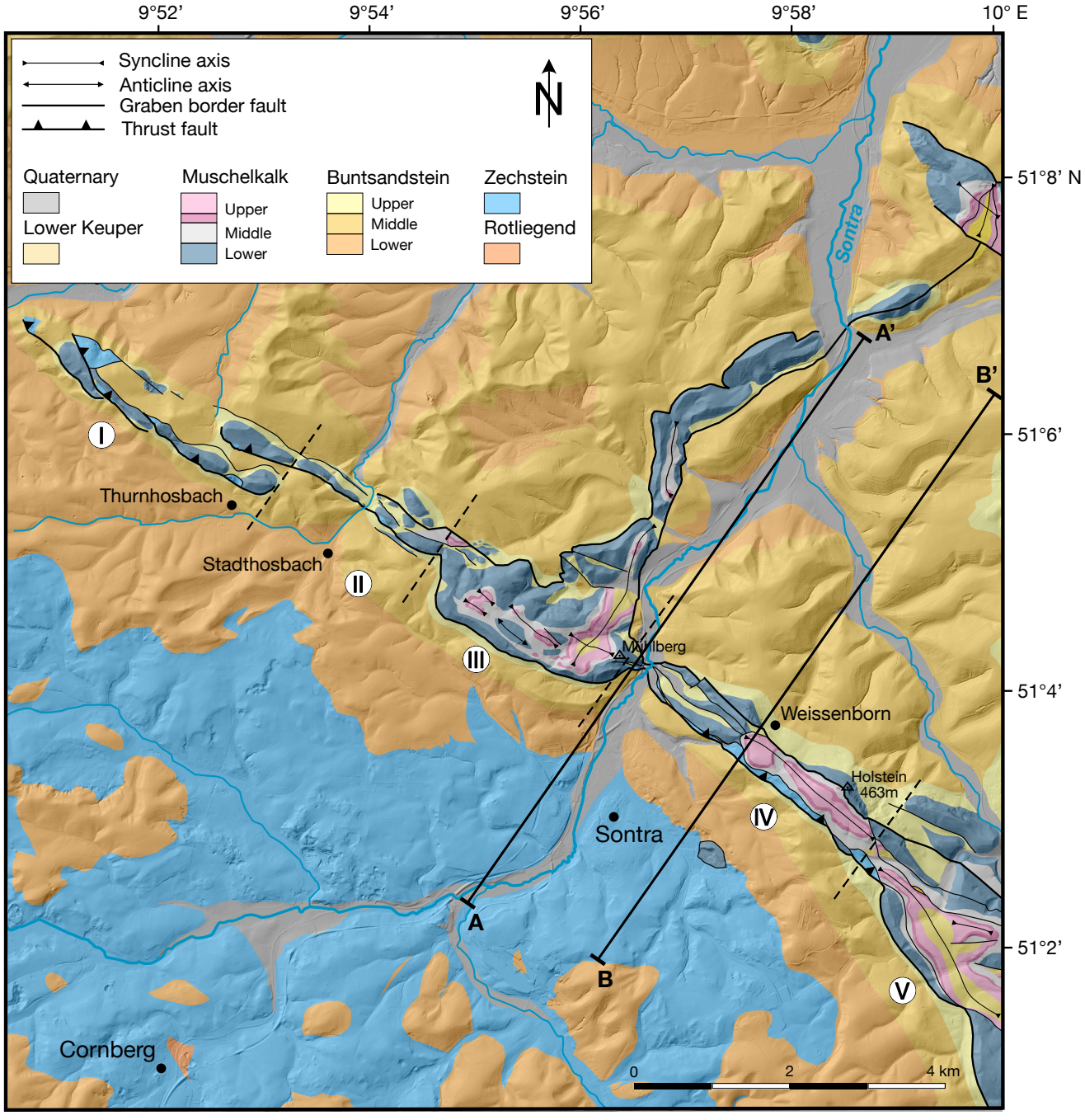

Figure 4: Geological map of the study area. Lines marked A-A’ and B-B’ indicate the position of the balanced cross sections in Fig. 6. Roman letters define sections of the graben between the dashed lines, which are refered to and further discussed in the text. DEM courtesy of Hessian Agency for Nature Conservation, Environment and Geology (HLNUG).

https://doi.org/10.5194/se-2020-133
Preprint. Discussion started: 17 August 2020

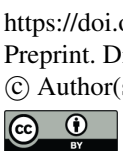

Solid Earth
Discussions
Open Access
EGU

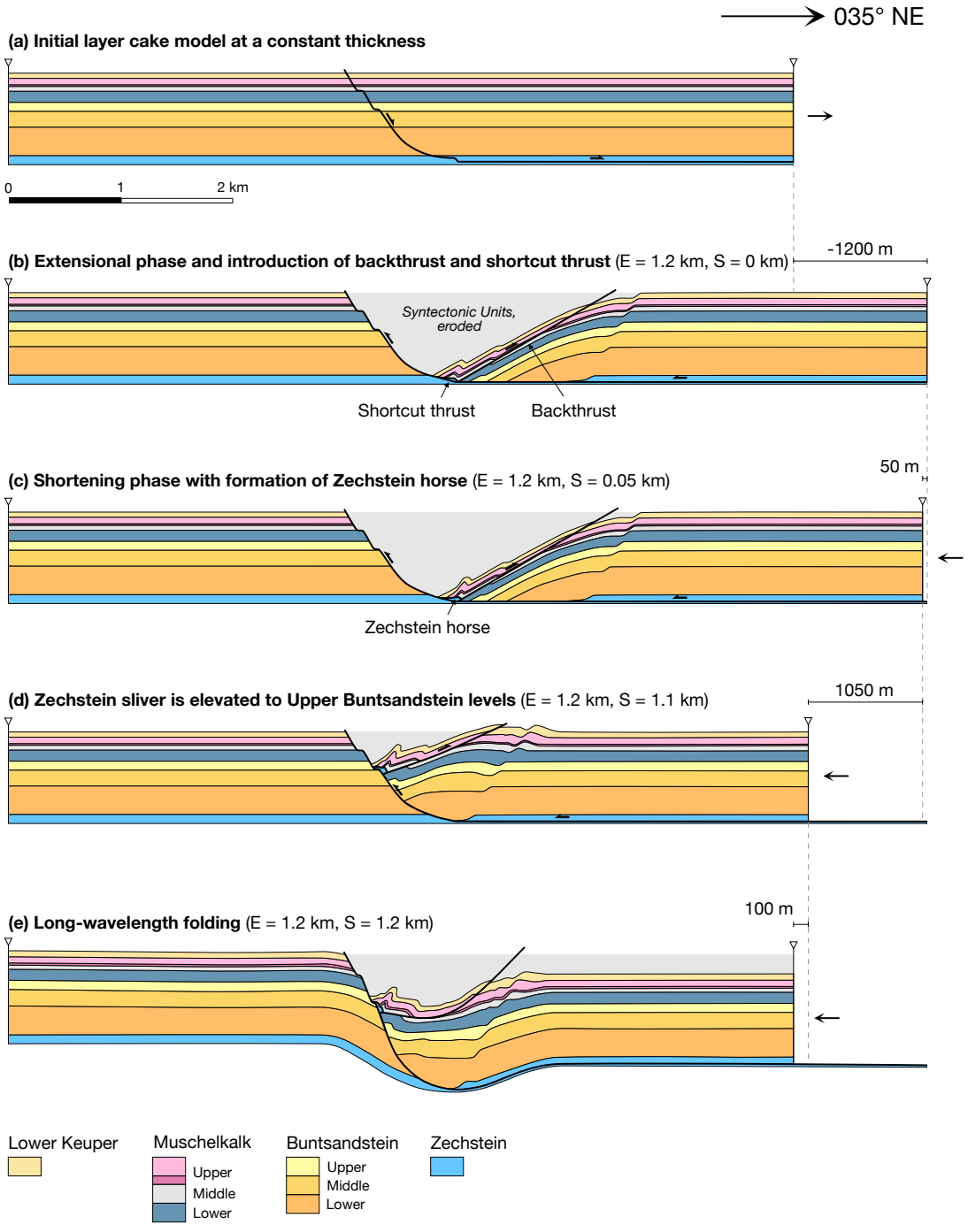

Figure 5: Forward model of the formation of the Sontra Graben. Stratigraphic thicknesses from Motzka-Noering et al. (1987).

https://doi.org/10.5194/se-2020-133
Preprint. Discussion started: 17 August 2020

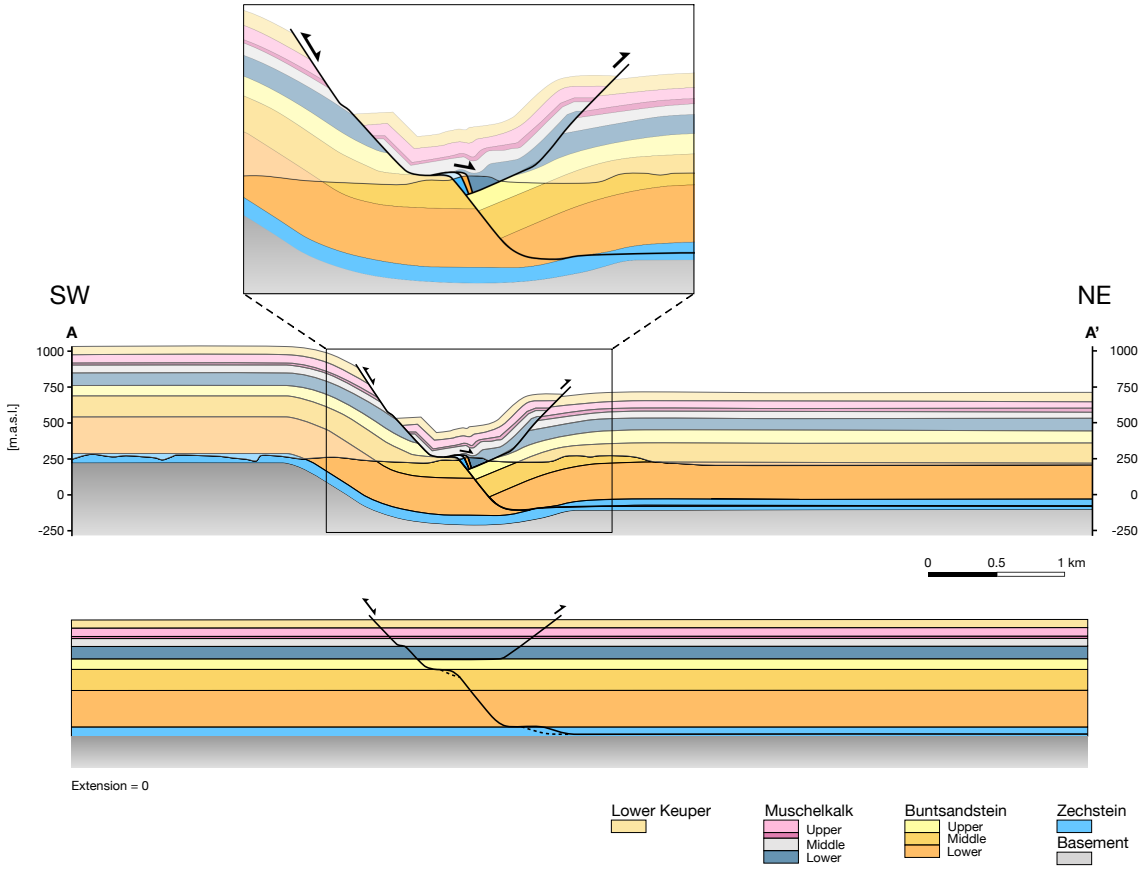

https://doi.org/10.5194/se-2020-133
Preprint. Discussion started: 17 August 2020

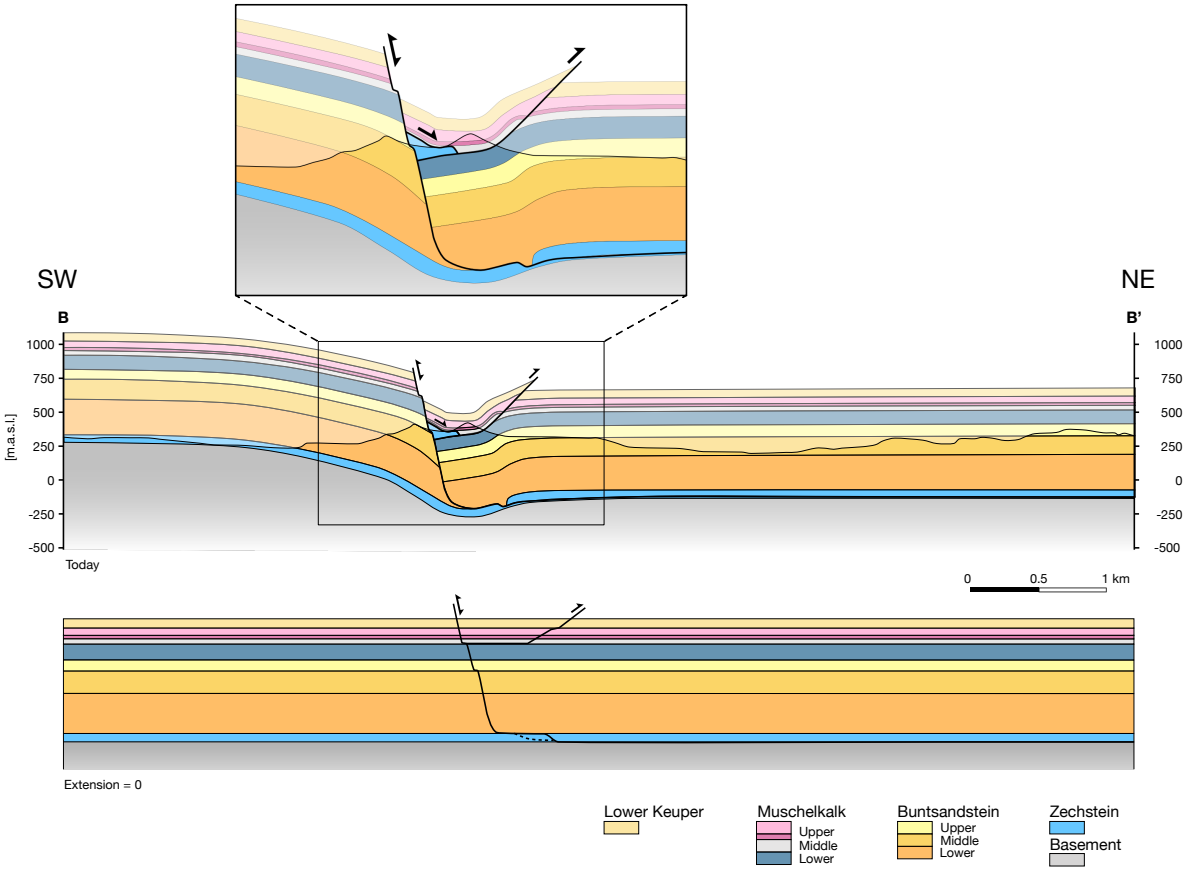

Figure 6: Balanced cross-sections of the Sontra Graben. The Fault geometry was verified through the forward model in Fig. 5. For section traces, see Fig. 4.

https://doi.org/10.5194/se-2020-133
Preprint. Discussion started: 17 August 2020

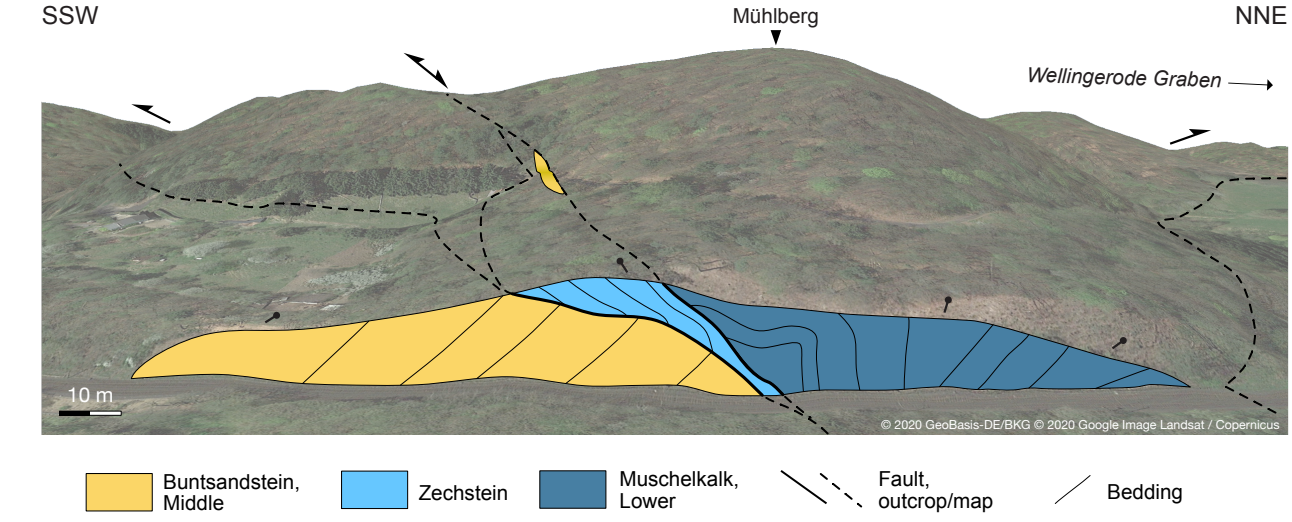

445

Figure 7: Outcrop on the train tracks near Sontra, previously documented by Schröder (1925). The outcrop shows the juxtaposition of one of the "exotic" Zechstein slivers, with circa fault parallel bedding, onto the Middle Buntsandstein of the graben shoulder. Position 51° 4'57.35"N, 9°56'24.49"E with view towards NNW. Image from Google, © 2020 GeoBasis-DE/BKG, © 2020 Google Image Landsat / Copernicus.

450

https://doi.org/10.5194/se-2020-133
Preprint. Discussion started: 17 August 2020

Solid Earth
Discussions
Open Access
EGU

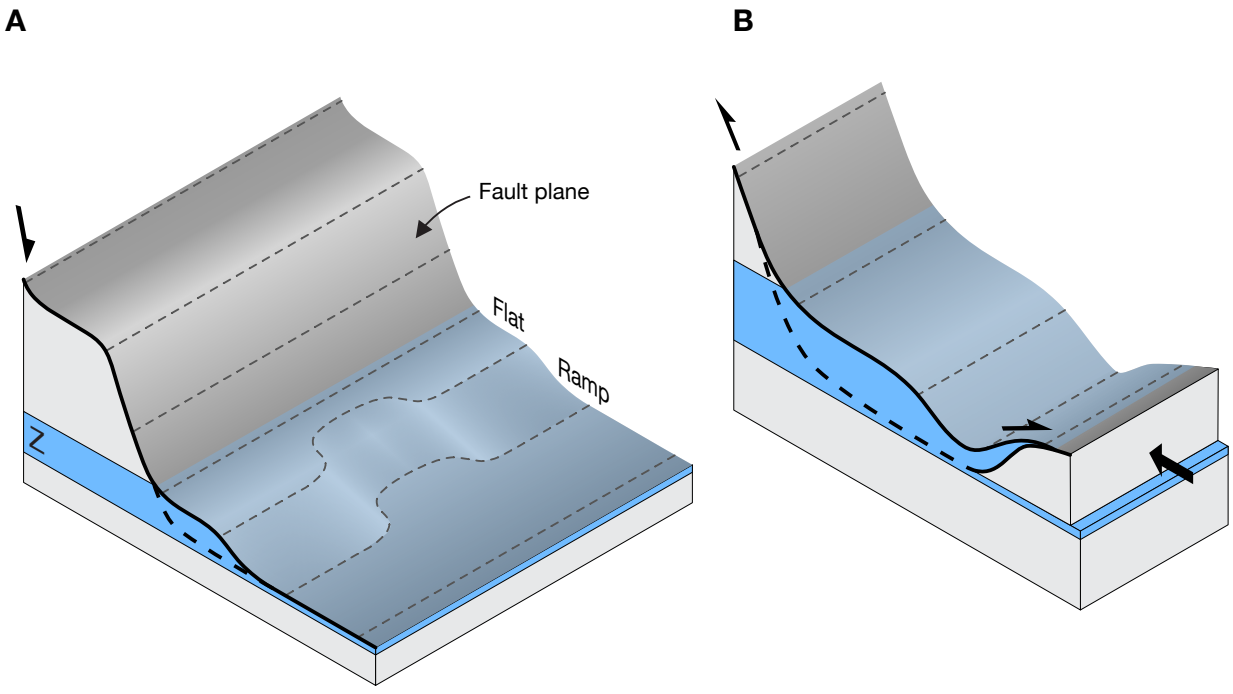

Figure 8: Schematic model of the formation of a horse and the backthrust onto the hanging wall during inversion. The slivers are formed as horses with the newly formed shortcut thrust as floor thrust and the original normal fault as roof thrust. (A) shows the geometry of the original normal fault with areas showing more or less pronounced development of flats. Areas with more pronounced flats produce the afore mentioned "exotic" slivers. Areas with less pronounced flats produce smaller or no slivers. (B) shows the newly formed sliver being backthrust onto the hanging wall during the inversion phase.

https://doi.org/10.5194/se-2020-133
Preprint. Discussion started: 17 August 2020

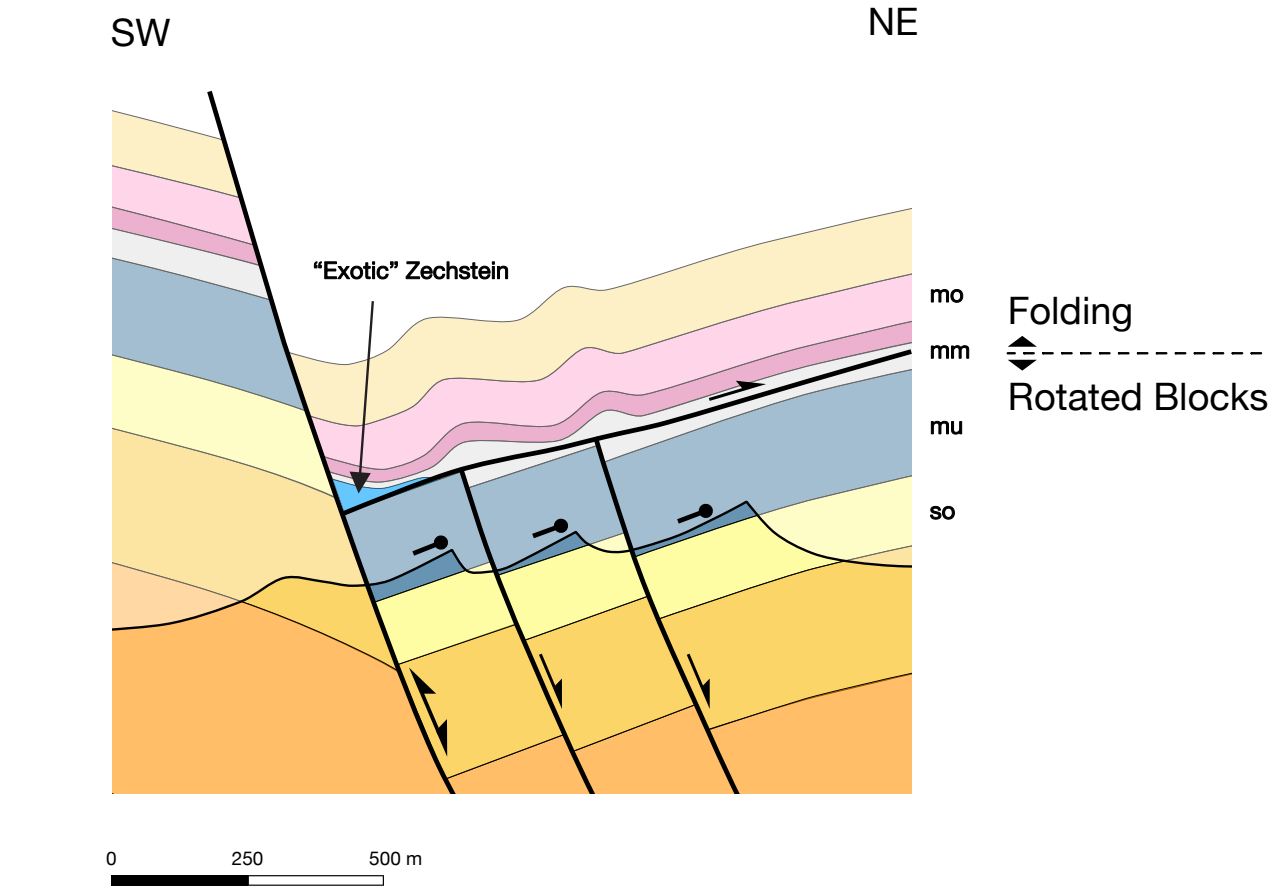

Figure 9: Schematic model of the transition from the lower structural floor with rotated blocks to the upper structural floor dominated by folding as a result of a detachment within the Middle Muschelkalk. Faults delimiting the rotated blocks within the lower floor peter out into the Middle Muschelkalk. Through varying degrees of erosion the different styles become visible in the different section of the map.

https://doi.org/10.5194/se-2020-133
Preprint. Discussion started: 17 August 2020

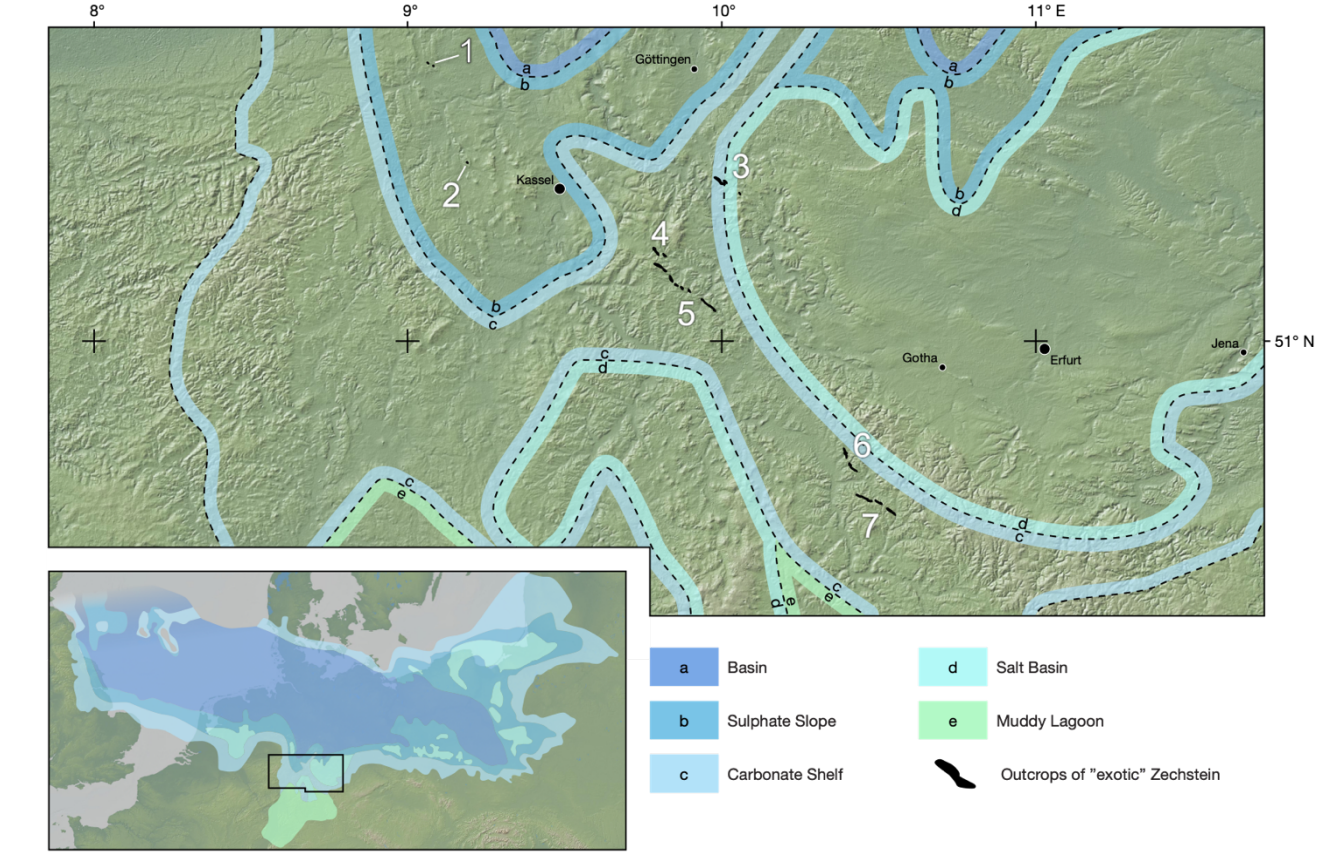

460

Figure 10: Paleogeographic map of the first Zechstein cycle (Z1, Werra cycle). Outcrops of "exotic" Zechstein are shown in black for better visibility. Locality 5 is the subject of this study. Zechstein paleogeography from Kiersnowski et al., 1995. Digital elevation model made with GeoMapApp (www.geomapapp.org) / CC BY.

https://doi.org/10.5194/se-2020-133
Preprint. Discussion started: 17 August 2020

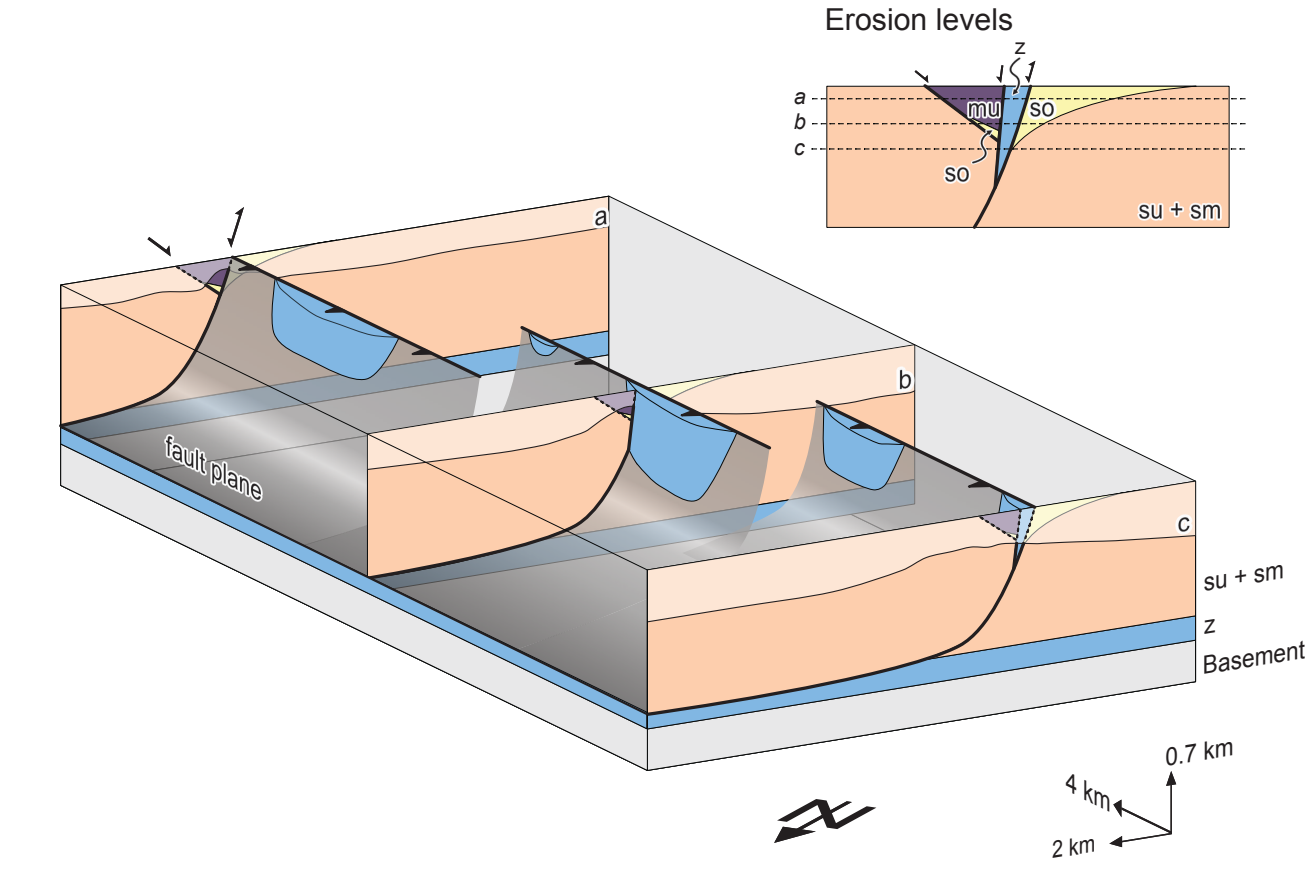

Figure 11: Schematic model for explaining the appearance of multiple rows of Zechstein slivers along imbricated faults as part of a transfer type structure, observed in the western part of the graben (section I, Fig. 4). Different erosion levels determine the width of the graben as it appears on the map.

https://doi.org/10.5194/se-2020-133
Preprint. Discussion started: 17 August 2020

Solid Earth
Discussions
Open Access
EGU

Table 1: Statistical compilation of the Zechstein slivers. The values for vertical offset are calculated based on thicknesses given by Motzka-Noering et al., (1987).

Zone	No.	Area [m²]	Long axes [m]	Short axes [m]	Strike (mean)	Dip (mean)	Stratigaphy	Bordering units		Vertical offset [m]	
								SW	NE	SW	NE
I	1	24,96	195	158	70	28	Plattendolomit	sm	sm	250	250
	2	100,33	500	290	131	56	Hauptdolomit	sm	mu	250	475
	3	6,909	172	50	35	45	n.a.	mu	so	475	395
	4	2,11	92	28	n.a.	n.a.	n.a.	mu	so	475	395
	5	963	50	28	n.a.	n.a.	n.a.	mu	so	475	395
	6	7,495	238	65	118	43	Hauptdolomit	sm	mu	250	475
	7	3,218	183	20	126	58	n.a.	mu	so	475	395
	8	1,521	125	17	135	59	n.a.	mu	so	475	395
	9	14,6	227	80	113	23	Plattendolomit	so, mu	so	475	395
	10	5,453	177	57	123	60	n.a.	mu	sm, so	475	395
II	11	1,327	95	21	145	29	n.a.	mu	so	475	395
	12	7,381	165	58	n.a.	n.a.	Hauptdolomit	mu	so	475	395
IV	13	8,778	255	46	117	27	n.a.	mu, sm	sm, so, mu	475	475
	14	3,84	153	28	n.a.	n.a.	n.a.	so	n.a.	395	n.a.
	15a	20,2	634	45	99	27	Anhydritknotensch.	mu	sm, so	475	395
	15b	128,66	1,458	98	136	40	Zechsteinkalk	mm	so	575	395
V	16	45,97	529	136	118	28	n.a.	mm, ku	so, mu	690	475
mean		22.571,47	308,71	72,06	114	43				446	416
median		7381,00	183,00	50,00	119	42				475	395